

Spectral measurement of the breakdown limit of β -Ga₂O₃ and field-dependent dissociation of self-trapped excitons and holes

Md Mohsinur Rahman Adnan^{1&}, Darpan Verma^{2&}, Zhanbo Xia¹, Nidhin Kumar Kalarickal¹,
Siddharth Rajan¹, Roberto C Myers^{1,2}

¹Department of Electrical and Computer Engineering, The Ohio State University, Columbus,
Ohio 43210, United States

²Department of Material Science and Engineering, The Ohio State University, Columbus, Ohio
43210, United States

Abstract:

Owing to its strong ionic character coupled with a light electron effective mass, β -Ga₂O₃ is an unusual semiconductor where large electric fields (~ 1 -6 MV/cm) can be applied while still maintaining a dominant excitonic absorption peak below its ultra-wide bandgap ($E_g \sim 4.9$ eV). This provides a rare opportunity in the solid-state to examine exciton and carrier self-trapping dynamics in a steady-state non-perturbative electric field. Under sub-bandgap photon excitation, we observe a field-induced red-shift of the spectral photocurrent peak associated with exciton absorption and threshold-like increase in peak amplitude at high-field associated with self-trapped hole ionization. The field-dependent spectral response is quantitatively fit with an eXciton-modified Franz-Keldysh (XFK) effect model, which includes the electric-field dependent exciton binding energy due to the quadratic Stark effect. A remarkable saturation of the spectral red-shift with reverse bias is observed exactly at the onset of dielectric breakdown providing a spectral means to detect and quantify the local electric field and dielectric breakdown behavior in β -Ga₂O₃. Additionally, the field-dependent responsivity provides insight to the photocurrent production pathway revealing the photocurrent contributions of self-trapped excitons (STXs) and self-trapped holes (STHs) in β -Ga₂O₃. We employ a quantum mechanical model of the field-dependent tunneling-dissociation of STX and field-ionization of STH in β -Ga₂O₃ to model the non-linear field-dependence of the photocurrent amplitude. Fitting to the data, we estimate an effective mass of valence band holes ($18.8m_0$) and an ultrafast self-trapping time of holes (0.125 fs) from the data indicating that minority-hole transport in β -Ga₂O₃ arises through field-ionization of STH. These results show that a quantitative understanding of sub-band-gap absorption and p-type transport in β -Ga₂O₃ must include field-dependent exciton dissociation and self-trapped hole ionization.

[&]These authors contributed equally to the work.

I. INTRODUCTION

The conversion of electromagnetic radiation (photon flux) into current density (charge flux) is of fundamental importance in all solid-state optoelectronics. An electron-hole pair is produced at the location of single photon absorption and therefore the mutual Coulombic bond between the photocarriers (exciton) must be broken (dissociation) before carrier separation and collection can take place. However, excitons are generally considered unimportant for understanding the room-temperature optoelectronic response in dominantly covalent (sp^3 bonded) crystalline semiconductors [1,2]. Traditionally called Wannier-Mott excitons [3,4], the small exciton binding energies ($E_X < 25$ meV) and small dielectric constant, K values combined with light effective masses ($m^* < 1$) of the host material lead to exciton Bohr radii typically spanning multiple nearest neighbor bond distances ($a_B > 1$ nm) and are assumed to be fully thermally or electrically dissociated in room temperature optoelectronics [2,5,6]. The opposite extreme occurs in strongly ionic solids where exciton absorption dominates the optical response with $E_X > 500$ meV and $a_B < 0.5$ nm [7,8]. However, ionic crystals with such strongly-bonded excitons can hardly be classified as semiconductors, e.g. alkali halides [9,10], with strong electron-lattice coupling strongly limiting charge transport (polarons) [11,12].

More recently, the emergence of two-dimensional (2D) semiconductors with sizable bandgaps and light masses, e.g. Transition Metal Dichalcogenides (TMDs), has demonstrated a new regime of exciton physics with simultaneously large E_X and a_B [13–16]. Under these conditions, room temperature optoelectronic properties are dominated by excitons near the band edge. Moreover, charged excitons known as trions become possible with interesting physics and potential optoelectronic applications [17–21]. By comparison with TMDs, the ultra-wide bandgap (~ 4.6 – 4.9 eV [22,23]) semiconductor β -Ga₂O₃ occupies a unique phase space among 3D excitonic systems with strong similarities to 2D materials, but with the added tunability associated with its high dielectric breakdown field limit (~ 6 – 8 MV/cm [22–24]) motivating its development for high-power high-field devices and solar-blind ultraviolet photodetectors [23,25–28]. Additionally, this provides a rare solid-state testbed to explore field-dependent excited state dynamics in a steady-state (non-perturbative) electric field, Fig. 1(a) and (b).

A. eXciton Franz-Keldysh (XFK) Effect

Band-to-band absorption itself is altered in the application of an electric field, characterized by a broadening of the absorption edge below the bandgap due to tunneling-assisted absorption, called the Franz-Keldysh (FK) effect [29,30], Fig. 1(c). In 1966, Aspnes [31] developed a quantitative model for the field-dependent absorption spectrum within the effective mass approximation. This model was applied by Maeda *et al.* to quantitatively model the absorption phenomenon at constant excitation wavelength with varying applied field in wide bandgap semiconductors like SiC and GaN based devices [32–35]. But the Aspnes model ignores exciton absorption and is only valid in GaN in a limited range of wavelengths and fields. Theoretical work by Dow and Redfield [36], Blossey [37], and Merkulov [38] showed that the electron-hole Coulombic bond (exciton) leads to a qualitatively distinct electro-absorption behavior from the FK effect, namely a sub-bandgap absorption peak that shifts under an applied field, which we refer to as the eXciton Franz Keldysh (XFK) effect, Fig. 1(c). Sub-bandgap absorption in GaN gives rise to excitons which must be dissociated before any photocurrent can be measured [39]. Exciton absorption was observed in the FK-effect in GaN [40,41], revealing an exciton peak structure near the band edge in GaN absorption spectra, which redshifts with increasing applied field. We recently reported the experimental observation and quantitative modeling of the XFK effect in the photocurrent spectral response of GaN [39], which demonstrates a spectral measurement of the local electric field and a route to develop all-optical electric field microscopy to explore breakdown physics and refine electrostatic modeling for high field devices. However, in the case of GaN, $E_x \sim 20.3\text{-}27\text{ meV}$ [39], is modest ($\sim k_B T$), and therefore the XFK peak is only resolvable at relatively low electric fields since the excitons are easily dissociated [40,41]. By contrast, excitons in TMDs and $\beta\text{-Ga}_2\text{O}_3$ fully dominate the sub-bandgap absorption, an effect accentuated in the latter by the weak band-to-band absorption of its indirect bandgap [42,43].

B. 2D Excitons in TMDs and $\beta\text{-Ga}_2\text{O}_3$

Because excitons are electrically neutral, photocurrent is only obtained from strongly bound excitons if a sufficiently large electric field is applied to dissociate them into mobile conduction band electrons and valence band holes via tunneling [44–48], illustrated in Fig. 1(a). The tunneling barrier height and width are modified by an expected increase in the binding energy with field due

to the Stark effect [13–15,40,41,49–51]. Such field ionization phenomena are well studied in organic semiconductors [51,52], but for inorganic solid-state systems were typically limited to discussion of impurity ionization in the low-field (perturbative) regime [40,41,48]. Only very recently have such high-field exciton-dissociation processes been described in a group of inorganic solid-state systems i.e. in TMD materials [13–15,49,50]. For example, in layered semiconductor WSe₂ with exciton binding energy $E_x = 170$ meV, the bias-dependent photocurrent amplitude was explained in terms of a Stark-modified exciton binding energy, see supplementary material of Ref. [14]. *Ab initio* Bethe-Salpeter equation (BSE) calculations could predict the bandgap correctly only if dielectric screening effects of several h-BN layers were included but failed to predict the correct E_x , while a screened Wannier-Mott model could explain the observed E_x . Previously, numerical and analytical models for quantitative field-induced dissociation rates for different TMDs had been proposed that demonstrated exciton dissociation in such materials to be largely dependent on the anisotropic dielectric screening environment [17,49,53] due to the bonding anisotropy [54–56]. As a result, the effective in-plane electron-hole interaction behaves as an unscreened $1/r$ potential of a Hydrogen atom over long range, but a weaker logarithmic divergence over short range, which weakens with increased screening [37,38]. More recently, a numerical model by Kamban and Pedersen treats excitons as 2D Hydrogen atoms confined in-plane within a given screening distance and shows success in describing field-induced exciton dissociation and Stark shift behavior for various TMDs [49].

We note that such 2D-like Hydrogenic excitons appear to be present in β -Ga₂O₃ as well. The optical anisotropy of β -Ga₂O₃ was demonstrated experimentally by Onuma *et al.*'s electro-reflectance study [43] and further *ab initio* calculations (DFT+GW) by Furthmüller *et al.* [59] showing that O²⁻ 2p valance band states (holes) of β -Ga₂O₃ couple with Ga³⁺ 4s conduction band states (electrons) forming anisotropic (2D-like) excitons; binding energies for $s - p_x$ (a-axis polarized) and $s - p_z$ (c-axis polarized) are ~ 0.3 eV larger than that along $s - p_y$ (b-axis polarized). Exciton wave functions in β -Ga₂O₃ therefore exhibit a 2D anisotropy; weakly bound with large wave functions along the b-axis [010], and tightly bound with small wave function within the ac-plane (010). This pseudo-2D behavior of excitons in β -Ga₂O₃ is further corroborated by BSE calculations of Varley and Schleife [42] showing a strong exciton absorption at lower

energy for photons polarized along a (x) or c (z) axis, compared with b (y) axis. Just like TMDs, a screened Mott-Wannier model for estimating correct $E_X = 270$ meV must be used for β -Ga₂O₃ [60]. Beschedt *et al.* showed that due to the strong exciton binding energy (larger than optical phonon energies), lattice screening of the electron-hole interaction is greatly reduced in comparison with what is expected from the static dielectric constant.

C. Exciton Stark effect and field-ionization of self-trapped holes in β -Ga₂O₃

Similar to TMDs, β -Ga₂O₃ exhibits a large E_X (~ 0.18 - 0.27 eV [60–62]) and anisotropic (2D-like) optical response as predicted from the BSE calculations of its absorption spectra by Varley and Schleife [42]. Due to the anisotropic dielectric environment, similarly large exciton polarizabilities (induced dipole) are expected [49] such that the exciton binding energy is strongly field dependent (Stark effect). But unlike TMDs and similar to polarons ubiquitous to many ionic materials [63], β -Ga₂O₃ exhibits carrier self-trapping, where due to the large effective mass of the holes, they are localized to a few bond distances and the presence of a photo-hole generates a strong lattice distortion. For example, a photo-hole localized on an O²⁻ site will push Ga³⁺ nearest neighbors outward and draw O²⁻ next nearest neighbors inwards, forming a trapping potential (~ 0.49 eV [64]) that localizes the hole even further. These self-trapped holes (STHs) are thought to limit the p-type conductivity in β -Ga₂O₃. The STHs together with free electrons form Self-Trapped eXcitons (STXs) which demonstrate high binding energy (~ 0.68 eV [64]) like alkali halide excitons. Yamaoka *et al.* observed STX and STH in the optical response of β -Ga₂O₃ [64–66]. These STXs and STHs must respectively be dissociated and field-ionized if photocurrent is to be obtained from β -Ga₂O₃ devices, Fig. 1(a). It is therefore essential to examine the applicability of well-established solid-state theories and assumptions, e.g. effective mass approximation, to characterize the photocarrier dynamics and optical transitions (dominated by excitons) in β -Ga₂O₃.

Here, we present measurements of β -Ga₂O₃ exciton absorption and dissociation processes in the high-field regime (1-6 MV/cm). A photocurrent spectral peak associated with exciton absorption, red shifts under reverse bias due to the field-dependent XFK effect. The spectral response is well explained by a quantitative model that necessarily includes the field-dependence of the exciton

binding energy, i.e. the quadratic Stark effect. The model predicts a continuous red shift of the exciton peak with field, however the data reveal a field-limit to the red shift due the onset of breakdown, in agreement with previously reported estimates (~ 6 MV/cm [23,24]). With the electric field calibrated based on the exciton peak position, we examine the photocurrent peak amplitude response as a function of applied field. A high-field threshold behavior is revealed, with a turn-on at ~ 4.5 MV/cm. Such behavior cannot be explained by the XFK model which predicts an exciton absorption peak reduction with field. Instead, the peak amplitude changes are due to a strongly field-dependent quantum efficiency (ratio of electron-hole collected to photons absorbed) associated with exciton dissociation and STH ionization processes. We adapt a field-ionization model of quasi-bound state tunneling to describe the exciton dissociation process in β -Ga₂O₃. Using literature values of minority carrier lifetimes and carrier mobilities we derive field-dependent rate equations for dissociation, ionization, and photo-carrier transport. The highly non-linear field-dependence of the photocurrent is fit using two free parameters: the valence band hole effective mass, and the self-trapping time of holes. The determined values agree with theoretical band structure estimates for the valence band effective mass [60,61] and recent ultrafast measurements of self-trapped holes [67].

II. FIELD-INDUCED RED-SHIFT OF EXCITON ABSORPTION PEAK:

Figure 1(b) shows the structure of β -Ga₂O₃ Schottky Barrier Diode (SBD) used for our study. Epitaxial growth of β -Ga₂O₃ is carried out using PAMBE (Riber MBE Control Solutions M7). Slightly Ga-rich growth conditions are used for the growth of β -Ga₂O₃ : at a Ga beam equivalent pressure (BEP) of 8×10^{-8} Torr, and oxygen pressure during growth of 1.5×10^{-5} Torr, plasma power of 300 W and $T_{sub} = 630^\circ\text{C}$ (pyrometer). The epitaxial structure for the SBD consists of a UID Ga₂O₃ layer of $1 \mu\text{m}$ thickness grown on a Sn: Ga₂O₃ (010) substrate [22,68] (Tamura). The Schottky top contacts are formed by evaporating a Ni/Au (30 nm/100 nm) metal stack while the ohmic bottom contacts are a Ti/Au (50 nm/100 nm) metal stack annealed at 470°C for 1 min. As shown in fig. 1 band diagram, the UID Ga₂O₃ layer has an average doping concentration of $5 \times 10^{17}/\text{cm}^3$, obtained from C-V measurements. Beyond the UID layer, the doping concentration is slightly higher i.e. $1 \times 10^{18}/\text{cm}^3$. The energy band diagram calculated from 1-D Poisson solver [69,70] in Fig. 1(b) demonstrates that almost all the applied potential drops within the $1 \mu\text{m}$ -

thick UID layer. The experimental setup for the photocurrent spectral measurement is the same as described in Ref. [39]. A chopped Xe-lamp coupled to a monochromator serves as the pulsed photo-excitation that is focused onto the SBD generating an alternating photocurrent, which is acquired with a lock-in amplifier.

Several photocurrent spectra for β -Ga₂O₃ SBD are shown in Fig. 2(a). The spectral variation in the absorption due to applied reverse bias (V_{exp}) is qualitatively different for the β -Ga₂O₃ device than what is observed in other wide bandgap semiconductors [33,39–41]. GaN p-n diodes show an XFK induced redshift of the optical absorption edge along with spectral broadening as bias increases [39]. This increased sub-band-gap absorption broadening is typical of the band edge FK-effect. In contrast, the β -Ga₂O₃ SBD shows an FK-like red shift of the eXciton peak with increasing bias, but without any apparent spectral broadening (inset of Fig. 2(a)). Moreover, the photocurrent peak increases with V_{exp} in a non-linear fashion for β -Ga₂O₃ SBD. By employing a Bi-Gaussian model [71] peak fitting routine, we extract the peak position (E_{ph}^0) and peak amplitude (I_{PR}^0) as a function of V_{exp} . The redshift of E_{ph}^0 with V_{exp} is clearly observed in Fig. 2(b) and the non-linear dependence of I_{PR}^0 on V_{exp} is shown in Fig. 2(c). These phenomena will be shown to arise from the field-dependent exciton binding energy and tunneling dissociation pathways, respectively.

A. Photoresponsivity and field-dependent absorption coefficient

To understand the photoresponsivity behavior, we note that the SBD is a vertical device with probes placed on the top and bottom metal electrodes. If the photon flux incident on the top electrode is φ_0 , then the flux entering β -Ga₂O₃ is $(1 - r)\varphi_0$, where r is the reflectance of the top electrode. After absorption in the depletion region, the photon flux exiting the depletion region and entering the non-depleted β -Ga₂O₃ is $(1 - r)\varphi_0 e^{-\int_0^W \alpha_{XFK}(F(z), \omega) dz}$, where $\alpha_{XFK}(F(z), E_{ph})$ is the field-dependent eXciton Franz Keldysh (XFK) absorption coefficient, $F(z)$ is the vertical component of the electric field versus depth (z), and W is the depletion width. Since the non-depleted layer has negligible electric field, photocarriers can only be produced and collected within the minority hole diffusion length, L_n , with an absorption factor of $e^{-\alpha_n L_n}$, where α_n is the absorption coefficient of n-doped β -Ga₂O₃. Because the absorption coefficient of β -Ga₂O₃ is quite

small in below band-gap photon energy range ($< 10^3/cm$) [72] and the minority hole diffusion length L_n is only $\sim 200-300nm$ [73], then $e^{-\alpha_n L_n} \sim 1.000$ and we can fully neglect photocurrent produced in this region. Absorption in the non-depleted n-type $\beta\text{-Ga}_2\text{O}_3$ layer and $500\ \mu m$ -reduces the photon flux incident on the back surface to $\sim e^{-\alpha_n L} > e^{-1000*0.05}$, which together with the diffuse hemispherical reflection off the back surface of the substrate allows us to ignore absorption due to a second optical pass through the depletion region. Within the depletion region of the Schottky diode where almost all the voltage drops, the absorbed photon flux (converted into excitons) is $(1-r)\varphi_0 \left(1 - e^{-\int_0^W \alpha_{XFK}(F(z), \omega) dz}\right)$. Thus, the photocurrent density generated in the SBD will be,

$$I_{PC} = \eta q (1-r) \varphi_0 \left(1 - e^{-\int_0^W \alpha_{XFK}(F(z), \omega) dz}\right) \quad \dots(1)$$

Where η is the internal quantum efficiency (IQE) representing the ratio of carriers collected to photons absorbed and q is the electron charge. Normalizing the photocurrent with respect to the measured wavelength dependent input power density ($E_{ph}(1-r)\varphi_0$) gives the photoresponsivity, I_{PR} (in A/W),

$$I_{PR} = \frac{I_{PC}}{E_{ph}(1-r)\varphi_0} = \frac{\eta q \left(1 - e^{-\int_0^W \alpha_{XFK}(F(z), \omega) dz}\right)}{E_{ph}} \quad \dots(2)$$

Thus, the photoresponsivity spectrum depends only on the average absorption coefficient in the depletion layer, the depletion width, and the quantum efficiency.

B. Stark-modified eXction Franz-Keldysh (XFK) effect in $\beta\text{-Ga}_2\text{O}_3$

$\beta\text{-Ga}_2\text{O}_3$ has an exciton binding energy $E_x^0 = 180-270\text{ meV}$ [60–62] at zero applied field ($F=0$). The binding energy increases with electric field due to the Stark effect, $E_x = E_x^0 + bF^2$, where $b = \frac{9q^2 a_B^2}{8E_x^0}$ is the polarizability [51]. Here, $a_B = a_0 K m_0 / \mu_{ex}$ is the exciton Bohr radius, a_0 ($\sim 53\text{ pm}$) is the Bohr radius of Hydrogen and $E_x^0 = 13.6 \mu_{ex} / (m_0 K^2)$, where μ_{ex} is the exciton reduced mass and K is the static dielectric constant, which strongly influences the polarizability b . Bechstedt *et al.* developed a modified-Wannier-Mott exciton model for $\beta\text{-Ga}_2\text{O}_3$ which

incorporates an effective dielectric constant ($K^* \sim 3.99$) that considers the LO-phonon charge carrier screening at optical frequencies and the anisotropic effective mass [60]. This modified-Wannier-Mott exciton model captures the experimentally determined values of E_x of β -Ga₂O₃. K (K^*) is the static (effective) dielectric constant which equals 14.82 (3.99) [60], $\mu_{ex} = 0.3m_0$ [60]. Using $a_B \sim 0.70$ nm, $E_x^0 \sim 250$ meV we calculate, $b = 2.1 \times 10^{-18} \text{ eV} \left(\frac{m}{V}\right)^2$, which is of the same order of magnitude as for several of the TMDs, see Table II of Ref. [49]. Note that the predicted Stark shift of β -Ga₂O₃ traverses a similar range as found in TMD materials for the range of applied fields (≤ 0.5 MV/cm) of Ref. [49].

The field-dependent exciton absorption coefficient, $\alpha_{XFK}(F(z), \omega)$, is given by Merkulov [38],

$$\alpha_{XFK}(F(z), \omega) = Cx/\pi^2(\delta^2 x^2 + 1), \quad \dots(3)$$

$$\text{with } x = \frac{8}{f} e^{\left\{ -\frac{4\Delta^{\frac{3}{2}}}{3f} - \frac{2}{\sqrt{\Delta}} \ln\left(\frac{8\Delta^{\frac{3}{2}}}{f}\right) \right\}}, \quad \delta = \Delta - 1 - \frac{9f^2}{2}, \quad f = \frac{qF(z)a_B}{E_x}, \quad \Delta = \frac{E_g - \hbar\omega}{E_x}$$

where C is a normalization constant which is the same as for the free carrier case [74], meaning it does not affect the peak shift. Employing this quantitative model, we utilize $E_g = 4.9$ eV [22], $E_x^0 = 270$ meV [61], $\mu_{ex} = 0.3 m_0$ [60] with $a_B \cong 0.70$ nm and $K^* = 3.99$ [60].

C. Spectral observation of the breakdown limit of β -Ga₂O₃

The electric field profile is well approximated by a triangle, typical for Schottky diodes,

$$F(z) = F_{max} \left(\frac{W-z}{W} \right) \quad \dots(4),$$

Where, W (in μm) is the depletion width given by $W = \frac{2(V+V_{bi})}{F_{max}}$, V is the applied reverse bias, $V_{bi} = \varphi_B - \frac{KT}{q} \log\left(\frac{N_c}{N_d}\right)$ is the built-in potential barrier of the Ni/Au/ β -Ga₂O₃ SBD, $\varphi_B = 1.23\text{V}$ [75] is the barrier height, $N_c = 3.72 \times 10^{18}/\text{cm}^3$ [76] is the effective density of states for the conduction band, $N_d = 5 \times 10^{17}/\text{cm}^3$ is the UID layer donor concentration, and F_{max} is the field

maximum at the Schottky junction. Due to electrostatic variation, it is possible that the field profile changes from the idealized picture, leading to varying F_{max} and/or V , thus we explore the spectral sensitivity of I_{PR} to such variations in the field profile. First, holding V constant, F_{max} is varied to change the field description $F(z)$ as shown in Fig. 3(a). Second, keeping F_{max} constant, V is varied, Fig. 3(b). For all field profiles, the depletion width is determined by the electrostatic requirement that $V = \int_0^W F(z)dz$.

Using Eqns. 2-4 the I_{PR} spectra are calculated assuming $\eta = 1$ and plotted in Figs. 3(c) and (d) for the two different electrostatic conditions shown in Fig. 3(a) and (b), respectively. First, we note that the Stark-modified XFK model of I_{PR} shows the peak-shaped spectrum for sub-bandgap energies, in agreement with the experimental data of β -Ga₂O₃ (Fig. 2(a)). In the case of varying F_{max} and constant V (Fig. 3(a)), the modeled I_{PR} spectra in Fig. 3(c) show a redshift of the I_{PR} peak with F_{max} . For the $F(z)$ profile of Fig. 3(b), where the F_{max} is constant (2 MV/cm) but V is adjusted from 10 V to 40 V, the I_{PR} spectra show no clear variation (Fig. 3(d)). Thus, the peak positions of the I_{PR} spectra (E_{ph}^0) depend solely on F_{max} and exhibit no dependence on V . This demonstrates that for β -Ga₂O₃ SBDs, the photocurrent spectra are apparently insensitive to absorption in the low field regions.

From the modeled spectra, we numerically determine the relationship between F_{max} and E_{ph}^0 in order to calibrate E_{ph}^0 as a spectral field-sensor. Peak position is determined by bi-Gaussian peak fits to the modeled I_{PR} spectra shown in Fig. 3(c), and the determined E_{ph}^0 values are plotted as a function of F_{max} in Fig. 3(e). This relation between E_{ph}^0 and F_{max} is used as a transfer function to convert the measured peak positions (Fig. 2(b)) to estimated F_{max} values, plotted as a function of the experimentally applied bias (V_{exp}) in Fig. 3(f). Remarkably, we see clear evidence of a field-limit from this spectral data; the spectrally determined value of F_{max} does not increase continuously with V_{exp} and reaches a saturated value precisely at the theoretical breakdown limit of β -Ga₂O₃ i.e. ~ 6 MV/cm [23,24]. Note that our analysis above made no assumptions about the

breakdown limit, and the field values in Fig. 3(f) are entirely based on the measured photocurrent spectra modeled using the XFK effect and the exciton parameters of β -Ga₂O₃ previously described.

Because the photocurrent is excited at the focal point of the optical excitation at a particular (x, y) position on the SBD surface, the observed saturation of F_{max} at $V_{exp} \sim 30$ V is a locally measured phenomenon. In this field range, where local field saturation is observed, near or at the onset of dielectric breakdown, the global device still has not exhibited any current spiking, which occurs in devices processed from this same wafer at $40 \text{ V} < V_{exp} < 60 \text{ V}$. At the (x, y) position of the I_{PR} measurements, the local F_{max} becomes constant with applied bias in the range $30 \text{ V} < V_{exp} < 40 \text{ V}$, and therefore F_{max} must necessarily be increasing in other regions of the device that have not yet reached the breakdown limit. Thus, this measurement is sensitive to local field non-uniformity and could be used to map out likely breakdown pathways without destroying devices.

III. NON-LINEAR FIELD-DEPENDENT PHOTOCURRENT AMPLITUDE

From Fig. 2(c) we observe that the responsivity peak amplitudes, (I_{PR}^0) from the measurement (in A/W) are smaller than reported in Refs. [27,28,77]. In these studies, the amplitudes are larger than what is allowed by the theoretical limit of photocurrent generation due to a proposed gain mechanism, where the Schottky barrier gets lowered by positive charge (self-trapped hole) build up at the metal/semiconductor interface [27,28]. The discussion of photoresponsivity in these works starts from free carriers i.e. electron and hole; and does not treat exciton absorption and dissociation. In these experiments the photo-excitation is modulated at a slow rate < 1 Hz, and the unusually large responsivities appear to charge-up over > 100 ms timescales. In our experiments we modulate the excitation at ~ 200 Hz to eliminate these slow dynamics. Under these conditions, the responsivities are well-below the theoretical limit, and we observe no evidence of the Schottky barrier modulation gain mechanism. The amplitude variation observed in our case is explained by a field-dependent η , discussed below, due to exciton dissociation and self-trapped hole ionization.

A. Field-dependent photocurrent production pathways: rate equations

The proposed photocurrent generation mechanism is illustrated in Fig. 4, with two possible pathways. Both paths begin by below bandgap photons absorbed in β -Ga₂O₃ producing free excitons (X) consisting of a conduction band electron and a valence band hole that are mutually bound by $E_X^0 = 180\text{-}270$ meV [60,61]. Due to the polaron formation affinity [63] and large effective mass [42,60,61] of holes, the photo-excited holes cause a lattice distortion that induces a short-range trapping potential for the holes, forming a STH within $\tau_{ST} < 0.5$ ps at 295 K [67]. Thus, X that are not dissociated (path 1) become STXs (path 2) consisting of a conduction band electron bound to an STH. The X can also recombine, but this time scale ($>1\mu\text{s}$) [66] is much greater than τ_{ST} due to the indirect bandgap, and therefore there is negligible X recombination, a conclusion also supported by the lack of any reports of free-X photoluminescence, i.e. lack of emission peak at ~ 4.6 eV range in β -Ga₂O₃. The fraction of X that dissociate into free carriers along path 1 is, therefore, $\eta_X = D_X / (D_X + \tau_{ST}^{-1})$, where D_X is the field-dependent tunneling dissociation rate of X.

In steady-state, charge neutrality requires that photoelectron and photohole currents be identical. Given the larger effective mass of holes than of electrons, we assume the photocurrent is limited by photohole collection. Free holes have an average mobility of $20 \text{ cm}^2/\text{Vs}$ as recently reported [78], which is consistent with earlier measurements of long minority hole diffusion lengths of $\sim 200\text{-}300$ nm [73]. With depletion widths of <1000 nm, the electron and hole drift times are <1 ps (assuming saturation velocities $\geq 10^6$ cm/s), while the free carrier recombination times are ~ 210 ps [73]. Thus, the collection efficiency of free electrons or holes is $\sim 100\%$ over the experimental field range, and the total quantum efficiency of path 1 is $\eta_1 = \eta_X = D_X / (D_X + \tau_{ST}^{-1})$.

The fraction of X that become STX along path 2, is $(1 - \eta_X)$. Within the STX, the large lattice distortion binds the hole by 490 meV [64], localizing it within a single bond distance centered over an oxygen anion, rendering it immobile [16,42,59,63]. As the total STX binding energy is 680 meV [64], within the STX quasiparticle the electron is bound to the STH by $(680-490) = 190$ meV. As this energy is much smaller than the STH binding energy, the STX dissociation occurs by the electron tunneling into the conduction band at a field-dependent rate of D_{STX} . The fraction of STX

that are dissociated is, $\eta_{STX} = D_{STX}/(D_{STX} + R_{STX})$, where R_{STX} is the STX recombination rate ($\sim 10^6 \text{ s}^{-1}$) [66]. To produce any current in steady-state, the remaining STH must be field-ionized (490 meV) at a rate of D_{STH} in order to generate mobile free holes at an efficiency of $\eta_{STH} = D_{STH}/(D_{STH} + R_{STH})$. The total fraction of X that become STX and subsequently contribute to current (path 2) is thus, $\eta_2 = (1 - \eta_X) * \eta_{STX} * \eta_{STH}$.

To validate this model, a relationship between F and η is derived and compared with the measured I_{PR}^0 . From the spectral E_{ph}^0 data combined with the Stark-modified XFK model, a relation between V_{exp} and F_{max} was previously established, Fig. 3(f). Utilizing this relation, the I_{PR}^0 data in Fig. 2(c) are re-plotted as a function of F_{max} in Fig. 5(a). A sudden, threshold-like increase of amplitude at about $\sim 4.5 \text{ MV/cm}$ is observed. The total IQE is $\eta = \eta_1 + \eta_2$. However, if we assume that $\tau_{ST} = 0.5 \text{ ps}$ [67], then $\eta_1 \gg \eta_2$ over the entire field range and negligible current would be produced along path 2 at all field values. The data in Fig. 5(a) indicate this is not the case. We hypothesize that the X dissociation (path 1) dominates the photocurrent generation in $\beta\text{-Ga}_2\text{O}_3$ at lower fields, and the STX dissociation plus STH field-ionization (path 2) must dominate at higher fields i.e. η_2 turns-on at $\sim 4.5 \text{ MV/cm}$.

B. Field-dependent tunneling: exciton dissociation and self-trapped-hole ionization rates

The field-induced exciton dissociation and hole ionization rates (D_X, D_{STX}, D_{STH}) are quantitatively modeled utilizing the field-ionization model of impurities proposed by Chaudhuri *et al.* [79,80]. We note the astonishing similarities of $\beta\text{-Ga}_2\text{O}_3$ excitons (a light electron bound to a very heavy self-trapped hole) with hydrogenic impurities treated by Chaudhuri *et al.*'s model. Indeed, the exciton dissociation problem was treated previously with models [45,81,82] that match the hydrogenic exciton picture [83]. The field-dependent dissociation/ionization rate due to tunneling is given by,

$$D(F) = \omega \left(\frac{\alpha}{F}\right)^{2n^*-1} e^{-\frac{\alpha}{F}} \dots (5) \quad ,$$

Where n^* is the effective principle quantum number of the ground state within quantum defect theory, and,

$$\alpha = \frac{4 (2m^*)^{1/2} E_B^{3/2}}{3q\hbar}$$

$$\omega = \frac{6^{2n^*} E_B |s(n^*)|^2}{3\hbar\Gamma^2(n^* + 1)}$$

$$|s(n^*)| = \frac{\pi}{\sin(n^*\pi)} \left(\frac{1}{2} \sum_{m=0}^{\infty} \frac{1}{(n^* - m - 1)^2 (n^* - m)^2} \right)^{-1/2}$$

The reduced/effective mass (μ_{ex} , m_e , or m_h) is m^* and F is set equal to F_{max} . One should note that, unlike the Merkulov model, the Chaudhuri model incorporates the Stark effect [84]. Thus, incorporating the bF^2 term in E_B would be redundant, i.e. $E_B = E_x^0$. The non-integer effective principle quantum number (n^*) corrects for deviations from the purely hydrogenic case ($n^* = 1$), and is estimated by [80]:

$$E_B[eV] = \frac{m^* 13.6}{m_0 (Kn^*)^2} \dots (6)$$

For X, with $E_B = E_x^0 = 270 \text{ meV}$ [60], $\mu_{ex} = 0.3m_0$ [60], and $K = 3.99$ [60], then $n^* = 0.97$. In the case of the STX, replacing $E_B = E_x^0 = 680 - 490 = 180 \text{ meV}$ [65,66], then $n^* = 1.16$. Both values of n^* are fairly minor deviations from ideal hydrogenic states, which is consistent with X and STX Bohr radii ($a_B = 0.70 \text{ nm}$) that are several bond distances (0.19 nm) [85]. However, when the light electron is no longer present, as in the case of STHs, all that is left is the highly-localized heavy hole expected to exhibit deep-level behavior along with a local lattice distortion (polarization). In this case, an effective dielectric constant (K_{STH}) is not known, and neither is the effective mass of the host $\beta\text{-Ga}_2\text{O}_3$ valence band (m_h). In previous literature no conclusion could be drawn about its value except that it is $>10m_0$ [60,61].

There are several recent *ab initio* atomistic models of the STH in $\beta\text{-Ga}_2\text{O}_3$ that provide a definite length scale for the lattice distortion associated with the STH by calculating the probability density function of the hole, which occupies a p-orbital of an O^{2-} site [86–88]. From these calculations,

a_B of the STH is roughly half the average inter-ionic bond distance, indicating a strong departure from the hydrogenic cases of the X and STX. Guided by these first principles calculations, we consider $a_B = 0.06 - 0.14$ nm, which limits the range of $K_{STH} / m_h = 1.1 - 2.7$. Under this constraint, Eqns. 5-6 can be used to calculate D_{STH} with only one unknown parameter, m_h . As will be discussed below, good quality fits ($R^2 \geq 0.9$) are obtained for a range of $m_h = 18 - 25m_0$ for the considered range of a_B^* . However, the highest quality fit ($R^2 \sim 0.92$) is obtained for $m_h = 18.8m_0$, with $a_B^* = 0.127$ nm ($K_{STH} = 45$ and $n^* = 0.51$). The reduced n^* and increased K are consistent with a deep-level in a distorted dielectric environment.

Utilizing Eqn. (5) with $m_h = 18.8m_0$ ($n^* = 0.51$) and $\tau_{ST} = 0.125$ fs, D_X , D_{STX} , and D_{STH} as a function of F are calculated. The inverses of these rates, i.e. dissociation times, are plotted on a logarithmic scale in Fig. 5(b). Clearly D_{STH} (field-ionization of self-trapped holes) is the rate limiting process for photocurrent generation. We obtain quantum efficiencies for both paths (η_1 and η_2), plotted in the inset of Fig. 5(b). The rise in experimentally measured I_{PR}^0 at ~ 4.5 MV/cm is obtained by path 2's behavior (STX \rightarrow STH \rightarrow free carriers). Path 1 (X dissociation) dominates the photocurrent at low field, where the STH produced along path 2 cannot be ionized quickly enough to avoid recombination. But at sufficiently large fields, path 2 can contribute once D_{STH} outpaces R_{STH} .

The hole effective mass, m_h strongly impacts the tunneling rate of holes out of the self-trapping potential (Eqn. 5), and therefore m_h is well determined by the threshold field at which path 2 begins to contribute to photocurrent. This is illustrated in Fig. 5(c); keeping $\tau_{ST} = 0.125$ fs, if $m_h < 17.5m_0$, the path 2 turn-on happens too early (< 4 MV/cm), while for $m_h > 25.5m_0$ the turn-on happens too late (> 5 MV/cm). The best fit heavy hole mass ($m_h = 18.8m_0$) matches the observed I_{PR}^0 high-field turn-on at ~ 4.5 MV/cm.

The self-trapping time (τ_{ST}) of holes determines if any photocarriers can follow path 2 (i.e. η_1/η_2), and thus the ratio of the low field (path 1) and high-field (path 2) photocurrent magnitudes. This

is illustrated in Fig. 5(d); keeping $m_h = 20m_0$, if τ_{ST} is < 0.05 fs, the low-field photocurrent is too small, while if τ_{ST} is > 1 fs, then no high-field turn-on is observed. We note that the estimated $\tau_{ST} = 0.125$ fs is consistent with the ultrafast pump-probe absorption data in Ref. [67] taken at lower photon energies noting the time-resolution limitation of those experiments. Using this field-dependent model of η , Fig. 5(e) shows the modeled I_{PR} spectral behavior at varying F values. The calculated I_{PR}^0 values are normalized by the highest-field value and plotted as a function of F in Fig. 5(f). The model (line) shows a good match to the normalized data (points) taken from Fig. 5(a).

IV. CONCLUSIONS AND OUTLOOK

The optoelectronic properties of ultra-wide bandgap low-symmetry materials, like $\beta\text{-Ga}_2\text{O}_3$, are far less explored compared with other well-established semiconductors. Using a rather simple measurement (photocurrent spectroscopy in the sub-bandgap regime), a deeper understanding of electron-hole interaction at high electric field (strongly non-perturbative) was obtained. Just as in 2D TMDs [14,49], the electron-hole interaction in $\beta\text{-Ga}_2\text{O}_3$ takes on a 2D Hydrogen-like geometry leading to strong polarizabilities combined with large exciton binding energies. The result is that under large electric fields, the electron-hole interaction becomes even stronger, i.e. Stark effect, leading to a prominent redshift of the exciton absorption peak.

The exciton peak position was shown in $\beta\text{-Ga}_2\text{O}_3$ to serve as an accurate sensor of the electric field maximum in a Schottky diode structure. We observed a local electric field saturation effect, where the local field does not increase past ~ 6 MV/cm (nearly the breakdown field of $\beta\text{-Ga}_2\text{O}_3$) even though the experimentally applied bias increases (as does the photocurrent amplitude) indicating that this technique can be used to map out field non-uniformity and explore the onset of dielectric breakdown in a non-destructive manner, before actual device breakdown (current spiking) occurs.

Not only does this measurement provide a simple spectral means to track the local field, but the amplitude of the photocurrent versus electric field reveals a very unusual field-dependent quantum

efficiency. At $\sim 4.5 \text{ MV/cm}$, the peak amplitude shows an abrupt turn-on (threshold). This non-linear phenomenon is understood by developing the photocurrent rate equations for $\beta\text{-Ga}_2\text{O}_3$ considering the free exciton (X), self-trapped exciton (STX), and self-trapped hole (STH) field-dependent dissociation rates and ionization rates. As the excitons and STH in $\beta\text{-Ga}_2\text{O}_3$ are strongly bound, and the effective masses of holes are large, a deep-tunneling based field-ionization model was employed to model the ionization rates. Using literature values of the carrier lifetimes, the amplitude variation with field was fit to estimate two fundamental properties of the $\beta\text{-Ga}_2\text{O}_3$ valence band, the hole effective mass ($18.8m_0$) and the hole self-trapping time (0.125 fs) assuming an STH Bohr radius of 0.127 nm. Although this simplistic isotropic model ignores the anisotropy of the STH state, the results are consistent with previous atomistic *ab initio* studies, indicative of STH localized within 0.06 – 0.14 nm. Within the quantum effect theory, we find a reduced effective principle quantum number $n^* = 0.51$, which is consistent with the STH exhibiting deep-level character and an increased polarizability due to the local ionic distortion.

For a long time, non-perturbative high field exciton physics in 3D solids has evaded direct measurement and quantitative modeling. This is partly due to the scarcity of 3D materials with simultaneously large E_x and a_B , and partly due to limitations arising from smaller breakdown fields even when such materials can be found. As a result, this regime of exciton field-polarization physics was reported only for 1D quantum wires and more recently in 2D TMD materials [14,49,89]. Even then, the models could only qualitatively explain the results unless complex numerical methods were employed. However, in $\beta\text{-Ga}_2\text{O}_3$, the exciton Stark and Franz Keldysh phenomena can be explained using a simple modified-Wannier-Mott based model [38,39,80]. With the advent of a non-destructive optoelectronic method to measure electric field based on a spectral peak position, it may become more routine to quantify and study excitonic absorption and dissociation mediated photocurrent generation processes in semiconductors with strongly bound and anisotropic excitons.

Acknowledgments Funding for this research was provided by the Center for Emergent Materials: an NSF MRSEC under award number DMR-1420451 and by the AFOSR GAME MURI (Grant FA9550-18-1-0479, Program Manager Dr. Ali Sayir).

Figure Captions

Fig. 1: Electric-field modified exciton absorption, dissociation, and carrier ionization processes in the depletion region of a β -Ga₂O₃ Schottky barrier diode. (a) The photon flux is focused to a point (x, y) on the device surface, while an applied reverse bias and Schottky barrier cause a depleted region with a non-zero electric field (F) along the z -axis. Absorbed sub-bandgap photons generate neutral free eXcitons (X) formed by Coulombic electron and hole interaction and different ionization processes take place leading to photocurrent from drifting free carriers. F distorts the conduction band (CB) and valence band (VB) edges which allows e-tunneling based dissociation of X . Within X , holes generate a lattice distortion that locally binds holes generating neutral Self-Trapped eXcitons (STX), which themselves can dissociate by e-tunneling. Afterward, a Self-Trapped Hole (STH) is left behind. For these immobile charges to contribute to current, they must be field-ionized by h-tunneling out of the trapping potential. (b) Band edge diagram of the Schottky diode structure and layer structure. (c) Schematic of absorption coefficient (α) modified by F , the Franz-Keldysh effect. The sub-band-gap X absorption peak is red-shifted with the field, whereas the band edge absorption edge shows a field-induced broadening.

Fig. 2: (a) Photocurrent spectra normalized by excitation power (photoresponsivity I_{PR}) of a β -Ga₂O₃ Schottky barrier diode at various values of reverse bias (V_{exp}). Inset: the same data plotted on a semi-log scale. Grey points indicate the peak in I_{PR} . (b) Peak position (E_{ph}^0) as a function of V_{exp} displaying a redshift. (c) Peak amplitude (I_{PR}^0) as a function of V_{exp} displaying a non-linear increase.

Fig. 3: Spectral observation of the breakdown limit of β -Ga₂O₃ by local electric field (F) measurement. Two hypothetical electrostatic conditions are simulated. (a) Field profiles $F(z)$ at with varying peak field values (F_{max}), but with applied bias (V) held constant. (b) $F(z)$ with constant F_{max} , but varying V . (c) and (d) plot the photoresponsivity spectra modeled using Eqns. 2-4 (assuming $\eta = 1$) for the field profiles shown in (a) and (b), respectively. (e) Peak position (E_{ph}^0) extracted from the simulated spectra of (c) and plotted as a function of F_{max} demonstrating E_{ph}^0 as a spectral detector of F_{max} . (f) The data of Fig. 2(b) are replotted by using (e) as a transfer

function to convert the spectrally measured E_{ph}^0 values to estimated F_{max} values that are then plotted as a function of the experimentally applied reverse bias (V_{exp}). The spectrally estimated F_{max} saturates near the theoretical breakdown field of β -Ga₂O₃ before global device breakdown is observed.

Fig. 4: Photocurrent production pathways in β -Ga₂O₃ due to field-induced neutral free-eXciton (X) dissociation and carrier ionization processes. X dissociate at a rate D_X by e-tunneling into the conduction band (CB) generating free electrons and holes that drift to the electrodes along photocurrent path 1. Alternatively, holes can become self-trapped at a rate τ_{ST}^{-1} forming self-trapped eXcitons (STX), which themselves are dissociated by e-tunneling at a rate D_{STX} , otherwise, they recombine at a rate R_{STX} . If STX dissociate, they leave behind a Self-Trapped Hole (STH) that itself can either dissociate at a rate D_{STH} by h-tunneling into the valence band (VB), otherwise, they recombine with free-electrons at a rate R_{STH} . Path 1 is preferred at the low field with a probability of $\eta_1 = \eta_X$, while path 2 becomes possible at high-field with a probability of $\eta_2 = (1 - \eta_X) * \eta_{STX} * \eta_{STH}$.

Fig. 5: Field-dependent dissociation of self-trapped excitons and holes in β -Ga₂O₃. (a) Photoresponsivity peak amplitude (I_{PR}^0) as a function of field maximum (F_{max}) obtained by replotting the data of Fig. 2(c) and converting the experimental reverse bias to F_{max} using Fig. 3(f). (b) Dissociation times as a function of F calculated using Eq. 5. Inset: resulting quantum efficiencies of the two photocurrent production paths (see Fig. 4) as a function of F . The total quantum efficiency, η as a function of field F with varying (c) hole effective mass (m_h) and (d) self-trapping time (τ_{ST}) illustrating the sensitivity of the exciton and self-trapped hole field-ionization model to these material parameters. (e) Normalized photoresponsivity (I_{PR}^N) spectra at various F modeled using Eqns. 2-5, i.e. $\eta(F) \neq 1$. (f) Normalized I_{PR}^0 as a function of F comparing the data and the best fit. Data are from (a) and theory from (e), where the I_{PR}^0 are normalized by the maximum value of I_{PR}^0 .

References

- [1] E. M. L. D. De Jong, H. Rutjes, J. Valenta, M. T. Trinh, A. N. Poddubny, I. N. Yassievich, A. Capretti, and T. Gregorkiewicz, *Thermally Stimulated Exciton Emission in Si Nanocrystals*, *Light Sci. Appl.* **7**, 17133 (2018).
- [2] G. G. Macfarlane, T. P. McLean, J. E. Quarrington, and V. Roberts, *Exciton and Phonon Effects in the Absorption Spectra of Germanium and Silicon*, *J. Phys. Chem. Solids* **8**, 388 (1959).
- [3] G. H. Wannier, *The Structure of Electronic Excitation Levels in Insulating Crystals*, *Phys. Rev.* **52**, 191 (1937).
- [4] N. F. Mott, *On the Absorption of Light by Crystals*, *Proc. R. Soc. A* **167**, 384 (1938).
- [5] K. L. Shaklee and R. E. Nahory, *Valley-Orbit Splitting of Free Excitons? The Absorption Edge of Si*, *Phys. Rev. Lett.* **24**, 942 (1970).
- [6] T. P. McLean and R. Loudon, *Exciton Energy Levels in Germanium and Silicon*, *J. Phys. Chem. Solids* **13**, 1 (1960).
- [7] J. Frenkel, *On Pre-Breakdown Phenomena in Insulators and Electronic Semi-Conductors [3]*, *Phys. Rev.* **54**, 647 (1938).
- [8] N. Itoh and K. Tanimura, *Radiation Effects in Ionic Solids*, *Radiat. Eff.* **98**, 269 (1986).
- [9] R. T. Williams and M. N. Kabler, *Excited-State Absorption Spectroscopy of Self-Trapped Excitons in Alkali Halides*, *Phys. Rev. B* **9**, 1897 (1974).
- [10] D. Frohlich and B. Staginnus, *New Assignment of the Band Gap in the Alkali Bromides by Two Photon Spectroscopy*, *Phys. Rev. Lett.* **19**, 496 (1967).
- [11] M. Inoue, C. K. Mahutte, and S. Wang, *Electronic Polarons in Alkali Halides*, *Phys. Rev. B* **2**, 539 (1970).
- [12] J. T. Devreese, A. B. Kunz, and T. C. Collins, *A Resonance of the Electronic Polaron Appearing in the Optical Absorption of Alkali Halides*, *Solid State Commun.* **11**, 673 (1972).

- [13] B. Scharf, T. Frank, M. Gmitra, J. Fabian, I. Žutić, and V. Perebeinos, *Excitonic Stark Effect in MoS₂ Monolayers*, Phys. Rev. B **94**, 1 (2016).
- [14] M. Massicotte, F. Vialla, P. Schmidt, M. B. Lundeborg, S. Latini, S. Hastrup, M. Danovich, D. Davydovskaya, K. Watanabe, T. Taniguchi, V. I. Fal’ko, K. S. Thygesen, T. G. Pedersen, and F. H. L. Koppens, *Dissociation of Two-Dimensional Excitons in Monolayer WSe₂*, Nat. Commun. **9**, 1 (2018).
- [15] S. Hastrup, S. Latini, K. Bolotin, and K. S. Thygesen, *Stark Shift and Electric-Field-Induced Dissociation of Excitons in Monolayer MoS₂ and h-BN/ MoS₂ Heterostructures*, Phys. Rev. B **94**, 1 (2016).
- [16] G. Wang, A. Chernikov, M. M. Glazov, T. F. Heinz, X. Marie, T. Amand, and B. Urbaszek, *Colloquium: Excitons in Atomically Thin Transition Metal Dichalcogenides*, Rev. Mod. Phys. **90**, 21001 (2018).
- [17] Y. Lin, X. Ling, L. Yu, S. Huang, A. L. Hsu, Y. H. Lee, J. Kong, M. S. Dresselhaus, and T. Palacios, *Dielectric Screening of Excitons and Trions in Single-Layer MoS₂*, Nano Lett. **14**, 5569 (2014).
- [18] J. Pei, J. Yang, R. Xu, Y. H. Zeng, Y. W. Myint, S. Zhang, J. C. Zheng, Q. Qin, X. Wang, W. Jiang, and Y. Lu, *Exciton and Trion Dynamics in Bilayer MoS₂*, Small **11**, 6384 (2015).
- [19] C. Yang, Y. Gao, C. Qin, X. Liang, S. Han, G. Zhang, R. Chen, J. Hu, L. Xiao, and S. Jia, *All-Optical Reversible Manipulation of Exciton and Trion Emissions in Monolayer WS₂*, Nanomaterials **10**, (2020).
- [20] J. Yang, R. Xu, J. Pei, Y. W. Myint, F. Wang, Z. Wang, S. Zhang, Z. Yu, and Y. Lu, *Optical Tuning of Exciton and Trion Emissions in Monolayer Phosphorene*, Light Sci. Appl. **4**, 1 (2015).
- [21] C. H. Lui, A. J. Frenzel, D. V. Pilon, Y. H. Lee, X. Ling, G. M. Akselrod, J. Kong, and N. Gedik, *Trion-Induced Negative Photoconductivity in Monolayer MoS₂*, Phys. Rev. Lett. **113**, 1 (2014).
- [22] H. Masataka, S. Kohei, M. Hisashi, K. Yoshinao, K. Akinori, K. Akito, M. Takekazu, and

- Y. Shigenobu, *Recent Progress in Ga₂O₃ Power Devices*, Semicond. Sci. Technol. **31**, 34001 (2016).
- [23] X. Yan, I. S. Esqueda, J. Ma, J. Tice, and H. Wang, *High Breakdown Electric Field in β -Ga₂O₃/Graphene Vertical Barristor Heterostructure*, Appl. Phys. Lett. **112**, 1 (2018).
- [24] K. D. Chabak, N. Moser, A. J. Green, D. E. Walker, S. E. Tetlak, E. Heller, A. Crespo, R. Fitch, J. P. McCandless, K. Leedy, M. Baldini, G. Wagner, Z. Galazka, X. Li, and G. Jessen, *Enhancement-Mode Ga₂O₃ Wrap-Gate Fin Field-Effect Transistors on Native (100) β -Ga₂O₃ Substrate with High Breakdown Voltage*, Appl. Phys. Lett. **109**, (2016).
- [25] W. Y. Kong, G. A. Wu, K. Y. Wang, T. F. Zhang, Y. F. Zou, D. D. Wang, and L. B. Luo, *Graphene- β -Ga₂O₃ Heterojunction for Highly Sensitive Deep UV Photodetector Application*, Adv. Mater. **28**, 10725 (2016).
- [26] D. Guo, Q. Guo, Z. Chen, Z. Wu, P. Li, and W. Tang, *Review of Ga₂O₃-Based Optoelectronic Devices*, Mater. Today Phys. **11**, (2019).
- [27] A. Singh Pratiyush, S. Krishnamoorthy, S. Vishnu Solanke, Z. Xia, R. Muralidharan, S. Rajan, and D. N. Nath, *High Responsivity in Molecular Beam Epitaxy Grown β -Ga₂O₃ Metal Semiconductor Metal Solar Blind Deep-UV Photodetector*, Appl. Phys. Lett. **110**, 1 (2017).
- [28] A. S. Pratiyush, S. Krishnamoorthy, S. Kumar, Z. Xia, R. Muralidharan, S. Rajan, and D. N. Nath, *Demonstration of Zero Bias Responsivity in MBE Grown β -Ga₂O₃ Lateral Deep-UV Photodetector*, Jpn. J. Appl. Phys. **57**, (2018).
- [29] F. Walter, *Einfluß Eines Elektrischen Feldes Auf Eine Optische Absorptionskante*, Zeitschrift Fur Naturforsch. - Sect. A J. Phys. Sci. **13**, 484 (1958).
- [30] L. V Keldysh, *The Effect of a Strong Electric Field on the Optical Properties of Insulating Crystal*, J. Exptl. Theor. Phys. **34**, 1138 (1958).
- [31] D. E. Aspnes, *Electric-Field Effects on Optical Absorption near Thresholds in Solids*, Phys. Rev. **147**, 554 (1966).
- [32] T. Maeda, T. Narita, M. Kanechika, T. Uesugi, T. Kachi, T. Kimoto, M. Horita, and J.

- Suda, *Franz-Keldysh Effect in GaN p-n Junction Diode under High Reverse Bias Voltage*, Appl. Phys. Lett. **112**, (2018).
- [33] T. Maeda, X. Chi, H. Tanaka, M. Horita, J. Suda, and T. Kimoto, *Franz-Keldysh Effect in 4H-SiC p-n Junction Diodes under High Electric Field along the $\langle 1120 \rangle$ Direction*, Jpn. J. Appl. Phys. **58**, 0 (2019).
- [34] T. Maeda, T. Narita, H. Ueda, M. Kanechika, T. Uesugi, T. Kachi, T. Kimoto, M. Horita, and J. Suda, *Measurement of Avalanche Multiplication Utilizing Franz-Keldysh Effect in GaN p-n Junction Diodes with Double-Side-Depleted Shallow Bevel Termination*, Appl. Phys. Lett. **115**, (2019).
- [35] T. Maeda, X. Chi, M. Horita, J. Suda, and T. Kimoto, *Phonon-Assisted Optical Absorption Due to Franz-Keldysh Effect in 4H-SiC p-n Junction Diode under High Reverse Bias Voltage*, Appl. Phys. Express **11**, 0 (2018).
- [36] J. D. Dow and D. Redfield, *Electroabsorption in Semiconductors: The Excitonic Absorption Edge*, Phys. Rev. B (1970).
- [37] D. F. Blossey, *Wannier Exciton in an Electrical Field. I. Optical Absorption by Bound and Continuum States*, Phys. Rev. B **2**, 3976 (1970).
- [38] I. Merkulov, *Influence of Exciton Effect on Electroabsorption in Semiconductors*, Sov. J. Exp. Theor. Phys. **39**, 2314 (1974).
- [39] D. Verma, M. M. R. Adnan, M. W. Rahman, S. Rajan, and R. C. Myers, *Local Electric Field Measurement in GaN Diodes by Exciton Franz-Keldysh Photocurrent Spectroscopy*, Appl. Phys. Lett. **116**, 202102 (2020).
- [40] J. Y. Duboz, F. Binet, E. Rosencher, F. Scholz, and V. Härle, *Electric Field Effects on Excitons in Gallium Nitride*, Mater. Sci. Eng. B **43**, 269 (1997).
- [41] F. Binet, J. Duboz, E. Rosencher, F. Scholz, and V. Härle, *Electric Field Effects on Excitons in Gallium Nitride*, Phys. Rev. B **54**, 8116 (1996).
- [42] J. B. Varley and A. Schleife, *Bethe-Salpeter Calculation of Optical-Absorption Spectra of In_2O_3 and Ga_2O_3* , Semicond. Sci. Technol. **30**, (2015).

- [43] T. Onuma, K. Tanaka, K. Sasaki, T. Yamaguchi, T. Honda, A. Kuramata, S. Yamakoshi, and M. Higashiwaki, *Electroreflectance Study on Optical Anisotropy in β -Ga₂O₃*, Appl. Phys. Lett. **115**, (2019).
- [44] M. D. Tabak and P. J. Warter, *Field-Controlled Photogeneration and Free-Carrier Transport in Amorphous Selenium Films*, Phys. Rev. **173**, 899 (1968).
- [45] N. F. Mott and A. M. Stoneham, *The Lifetime of Electrons, Holes and Excitons before Self-Trapping*, J. Phys. C Solid State Phys. **10**, 3391 (1977).
- [46] S. D. Ganichev, I. N. Yassievich, and W. Prettl, *Tunnel Ionization of Deep Impurities by Far-Infrared Radiation*, Semicond. Sci. Technol. **11**, 679 (1996).
- [47] S. Ganichev, E. Ziemann, W. Prettl, and I. Yassievich, *Distinction between the Poole-Frenkel and Tunneling Models of Electric-Field-Stimulated Carrier Emission from Deep Levels in Semiconductors*, Phys. Rev. B **61**, 10361 (2000).
- [48] T. C. Smith, D.L., Pan, D.S., McGill, *Impact Ionization of Excitons in Ge and Si*, Phys. Rev. B **12**, (1975).
- [49] H. C. Kamban and T. G. Pedersen, *Field-Induced Dissociation of Two-Dimensional Excitons in Transition Metal Dichalcogenides*, Phys. Rev. B **100**, 1 (2019).
- [50] L. S. R. Cavalcante, D. R. Da Costa, G. A. Farias, D. R. Reichman, and A. Chaves, *Stark Shift of Excitons and Trions in Two-Dimensional Materials*, Phys. Rev. B **98**, 1 (2018).
- [51] G. Weiser, *Stark Effect of One-Dimensional Wannier Excitons in Polydiacetylene Single Crystals*, Phys. Rev. B **45**, 14076 (1992).
- [52] A. Horvath, G. Weiser, C. Lapersonne-Meyer, M. Schott, and S. Spagnoli, *Wannier Excitons and Franz-Keldysh Effect of Polydiacetylene Chains Diluted in Their Single Crystal Monomer Matrix*, Phys. Rev. B **53**, 13507 (1996).
- [53] S. Latini, T. Olsen, and K. S. Thygesen, *Excitons in van Der Waals Heterostructures: The Important Role of Dielectric Screening*, Phys. Rev. B **92**, 1 (2015).
- [54] L. Keldysh, *Coulomb Interaction in Thin Semiconductor and Semimetal Films*, Sov. J. Exp. Theor. Phys. Lett. **29**, 658 (1979).

- [55] H. I. Ralph, *The Electronic Absorption Edge in Layer Type Crystals*, Solid State Commun. **3**, 303 (1965).
- [56] M. Shinada and S. Sugano, *Interband Optical Transitions in Extremely Anisotropic Semiconductors I. Bound and Unbound Exciton Absorption*, J. Phys. Soc. Japan **21**, 1936 (1966).
- [57] P. Cudazzo, I. V. Tokatly, and A. Rubio, *Dielectric Screening in Two-Dimensional Insulators: Implications for Excitonic and Impurity States in Graphane*, Phys. Rev. B **84**, 1 (2011).
- [58] T. C. Berkelbach, M. S. Hybertsen, and D. R. Reichman, *Theory of Neutral and Charged Excitons in Monolayer Transition Metal Dichalcogenides*, Phys. Rev. B **88**, 1 (2013).
- [59] J. Furthmüller and F. Bechstedt, *Quasiparticle Bands and Spectra of Ga₂O₃ Polymorphs*, Phys. Rev. B **93**, 1 (2016).
- [60] F. Bechstedt and J. Furthmüller, *Influence of Screening Dynamics on Excitons in Ga₂O₃ Polymorphs*, Appl. Phys. Lett. **114**, 6 (2019).
- [61] A. Mock, R. Korlacki, C. Briley, V. Darakchieva, B. Monemar, Y. Kumagai, K. Goto, M. Higashiwaki, and M. Schubert, *Band-to-Band Transitions, Selection Rules, Effective Mass, and Excitonic Contributions in Monoclinic Ga₂O₃*, Phys. Rev. B **96**, (2017).
- [62] C. Sturm, J. Furthmüller, F. Bechstedt, R. Schmidt-Grund, and M. Grundmann, *Dielectric Tensor of Monoclinic Ga₂O₃ Single Crystals in the Spectral Range 0.5-8.5 eV*, APL Mater. **3**, 0 (2015).
- [63] J. B. Varley, A. Janotti, C. Franchini, and C. G. Van De Walle, *Role of Self-Trapping in Luminescence and p-Type Conductivity of Wide-Band-Gap Oxides*, Phys. Rev. B **85**, 2 (2012).
- [64] S. Yamaoka and M. Nakayama, *Evidence for Formation of Self-Trapped Excitons in a β -Ga₂O₃ Single Crystal*, Phys. Status Solidi **13**, 93 (2016).
- [65] S. Yamaoka, Y. Mikuni, and M. Nakayama, *Photoluminescence Polarization Characteristics of Self-Trapped Excitons in an Undoped β -Ga₂O₃ Single Crystal*, in

- Journal of Physics: Conference Series*, Vol. 1220 (Institute of Physics Publishing, 2019).
- [66] S. Yamaoka, Y. Furukawa, and M. Nakayama, *Initial Process of Photoluminescence Dynamics of Self-Trapped Excitons in a β -Ga₂O₃ Single Crystal*, Phys. Rev. B **95**, (2017).
 - [67] S. Marcinkevičius and J. S. Speck, *Ultrafast Dynamics of Hole Self-Localization in β -Ga₂O₃*, Appl. Phys. Lett. **116**, 2 (2020).
 - [68] M. Baldini, Z. Galazka, and G. Wagner, *Recent Progress in the Growth of β -Ga₂O₃ for Power Electronics Applications*, Mater. Sci. Semicond. Process. **78**, 132 (2018).
 - [69] B. Jogai, *Free Electron Distribution in AlGa_N/Ga_N Heterojunction Field-Effect Transistors*, J. Appl. Phys. **91**, 3721 (2002).
 - [70] M. Grundmann, *BandEng: Poisson-Schrodinger Solver Software*, <https://my.ece.ucsb.edu/mgrundmann/bandeng/>.
 - [71] E. Grushka, M. N. Meyers, and J. C. Giddings, *Moment Analysis for the Discern- Ment of Overlapping Chromatographic Peaks*, Anal. Chem. **42**, 21 (1970).
 - [72] H. Peelaers and C. G. Van De Walle, *Sub-Band-Gap Absorption in Ga₂O₃*, Appl. Phys. Lett. **111**, (2017).
 - [73] J. Lee, E. Flitsiyan, L. Chernyak, J. Yang, F. Ren, S. J. Pearton, B. Meyler, and Y. J. Salzman, *Effect of 1.5 MeV Electron Irradiation on β -Ga₂O₃ Carrier Lifetime and Diffusion Length*, Appl. Phys. Lett. **112**, (2018).
 - [74] H. Haug and S. W. Koch, *Quantum Theory Of The Optical And Electronic Properties Of Semiconductors*, 5th ed. (World Scientific Publishing Co., Singapore, 2004).
 - [75] H. Sheoran, B. R. Tak, N. Manikanthababu, and R. Singh, *Temperature-Dependent Electrical Characteristics of Ni/Au Vertical Schottky Barrier Diodes on β -Ga₂O₃ Epilayers*, ECS J. Solid State Sci. Technol. **9**, 055004 (2020).
 - [76] S. A. O. Russell, A. Perez-Tomas, C. F. McConville, C. A. Fisher, D. P. Hamilton, P. A. Mawby, and M. R. Jennings, *Heteroepitaxial Beta- Ga₂O₃ on 4H-SiC for an FET with Reduced Self Heating*, IEEE J. Electron Devices Soc. **5**, 256 (2017).

- [77] A. M. Armstrong, M. H. Crawford, A. Jayawardena, A. Ahyi, and S. Dhar, *Role of Self-Trapped Holes in the Photoconductive Gain of β -Gallium Oxide Schottky Diodes*, J. Appl. Phys. **119**, 1 (2016).
- [78] F. Akyol, *Simulation of β -Ga₂O₃ Vertical Schottky Diode Based Photodetectors Revealing Average Hole Mobility of 20 cm²V⁻¹s⁻¹*, J. Appl. Phys. **127**, (2020).
- [79] S. Chaudhuri, D. D. Coon, and G. E. Derkits, *Quantum-Mechanical Estimates of the Speed of Field Ionization of Shallow Impurity Levels*, Appl. Phys. Lett. **37**, 111 (1980).
- [80] S. Chaudhuri, D. D. Coon, and R. P. G. Karunasiri, *Impurity-to-Band Tunneling in Semiconductors*, J. Appl. Phys. **54**, 5476 (1983).
- [81] J. Singh, *Excitation Energy Transfer Processes in Condensed Matter Theory and Applications*, 1st ed. (Springer Science, Darwin, Australia, 1994).
- [82] J. Singh, *Optical Properties of Condensed Matter and Applications - Wiley Series in Materials for Electronic - Amp - Optoelectronic Applications*, 2nd ed. (JohnWiley & Sons Ltd, Darwin, Australia, 2006).
- [83] D. Farrelly and W. P. Reinhardt, *Uniform Semiclassical and Accurate Quantum Calculations of Complex Energy Eigenvalues for the Hydrogen Atom in a Uniform Electric Field*, J. Phys. B **16**, 2103 (1983).
- [84] J. R. Banavar, D. D. Coon, and G. E. Derkits, *Low-Temperature Field Ionization of Localized Impurity Levels in Semiconductors*, Appl. Phys. Lett. **34**, 94 (1979).
- [85] K. Irmscher, Z. Galazka, M. Pietsch, R. Uecker, and R. Fornari, *Crystal Structure of β -Ga₂O₃*, Cit. J. Appl. Phys. **110**, 676 (2011).
- [86] Y. K. Frodason, K. M. Johansen, L. Vines, and J. B. Varley, *Self-Trapped Hole and Impurity-Related Broad Luminescence in β -Ga₂O₃*, J. Appl. Phys. **127**, (2020).
- [87] T. Gake, Y. Kumagai, and F. Oba, *First-Principles Study of Self-Trapped Holes and Acceptor Impurities in Ga₂O₃ Polymorphs*, Phys. Rev. Mater. **3**, 44603 (2019).
- [88] B. E. Kananen, N. C. Giles, L. E. Halliburton, G. K. Foundos, K. B. Chang, and K. T. Stevens, *Self-Trapped Holes in β -Ga₂O₃ Crystals*, J. Appl. Phys. **122**, (2017).

- [89] T. G. Pedersen, *Analytical Models of Optical Response in One-Dimensional Semiconductors*, Phys. Lett. A **379**, 1785 (2015).

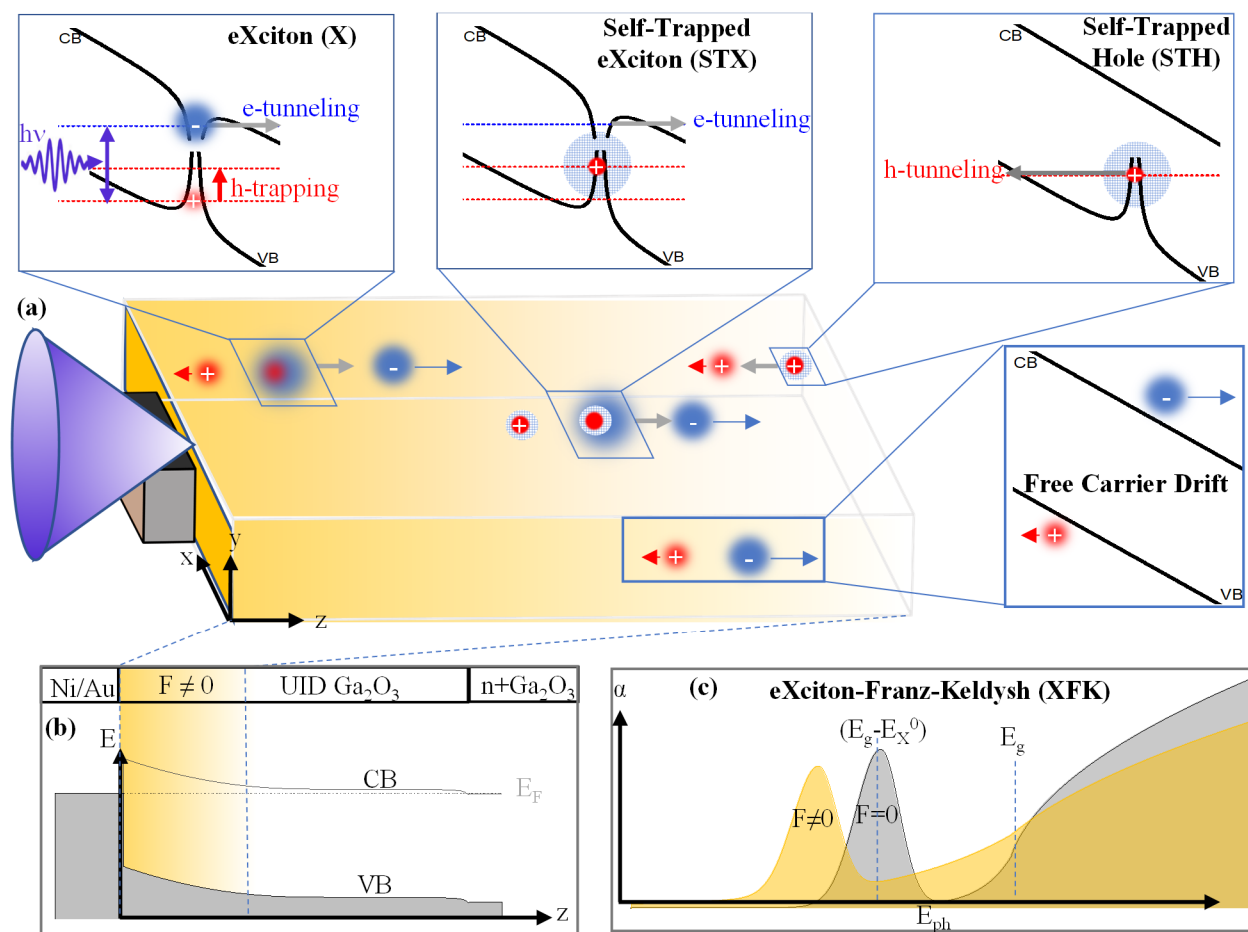


Fig. 1. Adnan *et al.*

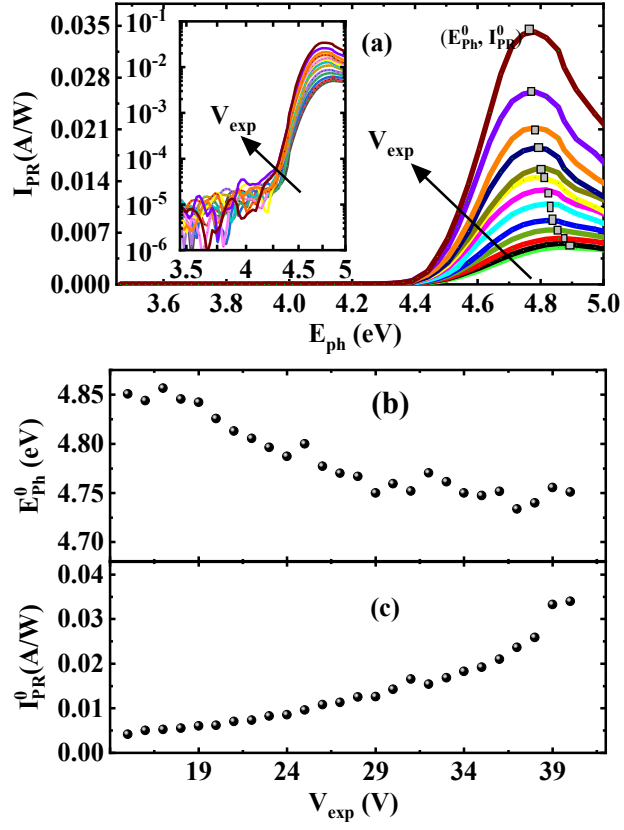


Fig. 2. Adnan *et al.*

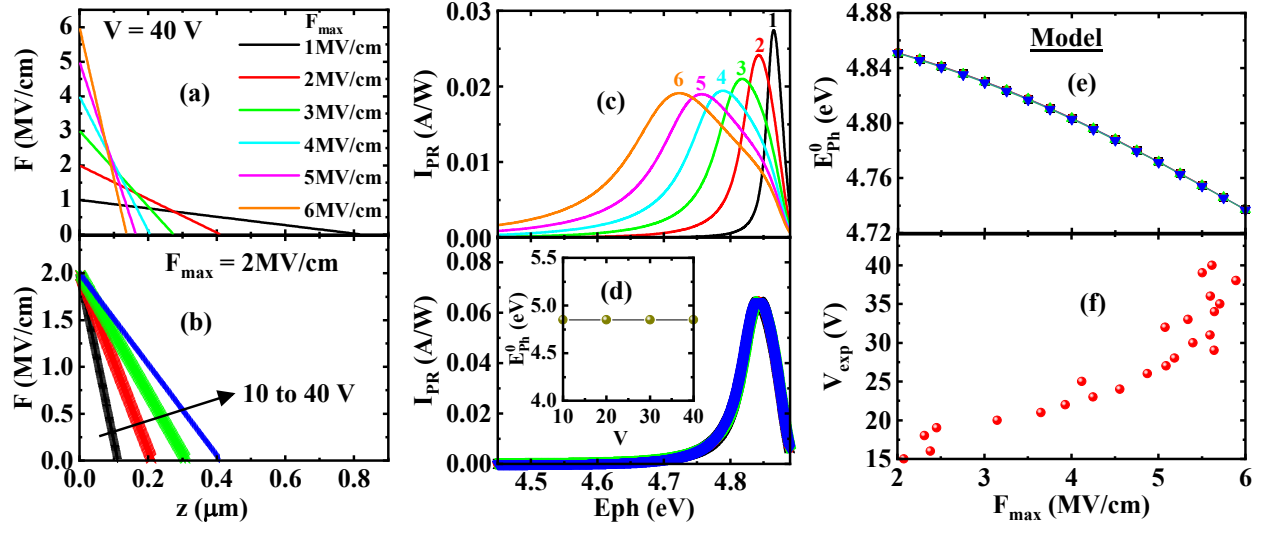


Fig. 3. Adnan *et al.*

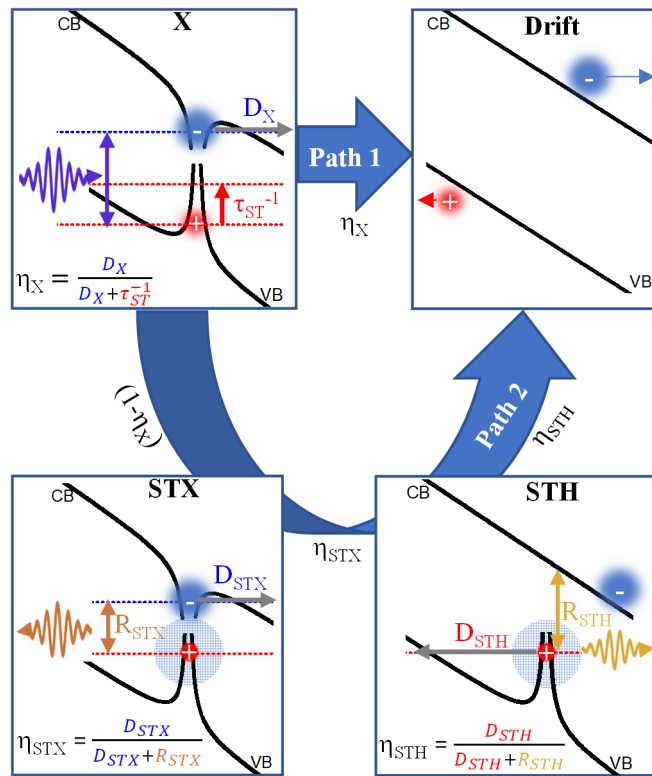


Fig. 4. Adnan *et al.*

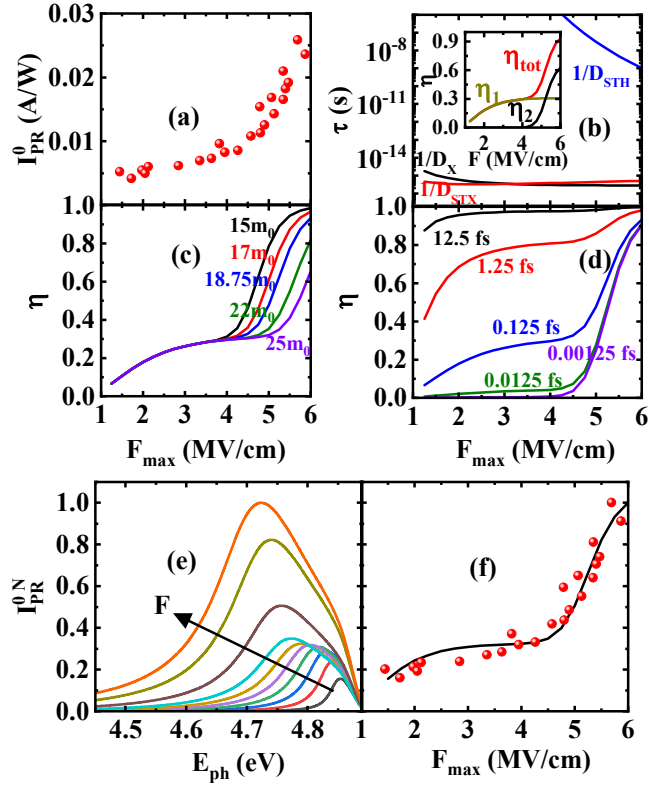


Fig. 5. Adnan *et al.*